

Supporting Information:
Interrogation of Base Pairing of the
Spiroiminodihydantoin Diastereomers Using the
 α -Hemolysin Latch

Tao Zeng, Aaron M. Fleming, Yun Ding, Henry S. White,* and Cynthia J. Burrows*

Department of Chemistry, University of Utah, 315 South 1400 East,
Salt Lake City, UT 84112-0850

*To whom correspondence should be addressed:

E-mail: burrows@chem.utah.edu or white@chem.utah.edu

Content	Page
Figure S1. HPLC chromatograms of the reaction mixture and the purified oligomers containing (S)-Sp or (R)-Sp.	S3
Figure S2. Uninterrupted $i-t$ trace and corresponding duration histogram for (S)-Sp:A-containing duplex in the α HL nanopore.	S4
Figure S3. Representative $i-t$ trace and current histogram for (S)-Sp:A-containing duplex in the α HL nanopore.	S5
Table S1. Current blocks normalized by the open channel current.	S6
Figure S4. Representative $i-t$ trace and current histogram for (R)-Sp:A-containing duplex in the α HL nanopore.	S7
Figure S5. Additional sample of $i-t$ trace for a mixture of (S)-Sp:A- and (R)-Sp:A-containing duplexes in the α HL nanopore.	S8
Figure S6. Representative $i-t$ trace and current histogram for (S)-Sp:A-containing duplex vs. the T:A internal standard in the α HL nanopore.	S9
Figure S7. Representative $i-t$ trace and current histogram for (R)-Sp:A-containing duplex vs. the T:A internal standard in the α HL nanopore.	S10

Figure S8. Representative $i-t$ trace for a mixture of (S)-Sp:G- and (R)-Sp:G-containing duplexes in the α HL nanopore. S11

Figure S9. Representative $i-t$ trace and current histogram for a mixture of (S)-Sp:T- and (R)-Sp:T-containing duplexes in the α HL nanopore. S12

Figure S10. Representative $i-t$ trace and current histogram for a mixture of (S)-Sp:C- and (R)-Sp:C-containing duplexes in the α HL nanopore. S13

Figure S11. Representative $i-t$ trace, current histogram, and current-noise density plot for (S)-Sp:G-containing duplex vs. the T:A internal standard in the α HL nanopore. S14

Figure S12. Representative $i-t$ trace, current histogram, and current-noise density plot for (R)-Sp:G-containing duplex vs. the T:A internal standard in the α HL nanopore. S15

Figure S13. Representative $i-t$ trace, current histogram, and current-noise density plot for (S)-Sp:T-containing duplex vs. the T:A internal standard in the α HL nanopore. S16

Figure S14. Representative $i-t$ trace, current histogram, and current-noise density plot for (R)-Sp:T-containing duplex vs. the T:A internal standard in the α HL nanopore. S17

Figure S15. Representative $i-t$ trace, current histogram, and current-noise density plot for (S)-Sp:C-containing duplex vs. the T:A internal standard in the α HL nanopore. S18

Figure S16. Representative $i-t$ trace, current histogram, and current-noise density plot for (R)-Sp:C-containing duplex vs. the T:A internal standard in the α HL nanopore. S19

Figure S17. Representative $i-t$ trace and current histogram for G:C-containing duplex vs. the T:A internal standard in the α HL nanopore. S20

Figure S18. Representative $i-t$ trace and current histogram for OG:C-containing duplex vs. the T:A internal standard in the α HL nanopore. S21

Figure S19. Melting curves for the duplexes containing G:C, (S)-Sp:C, or (R)-Sp:C base pair. S22

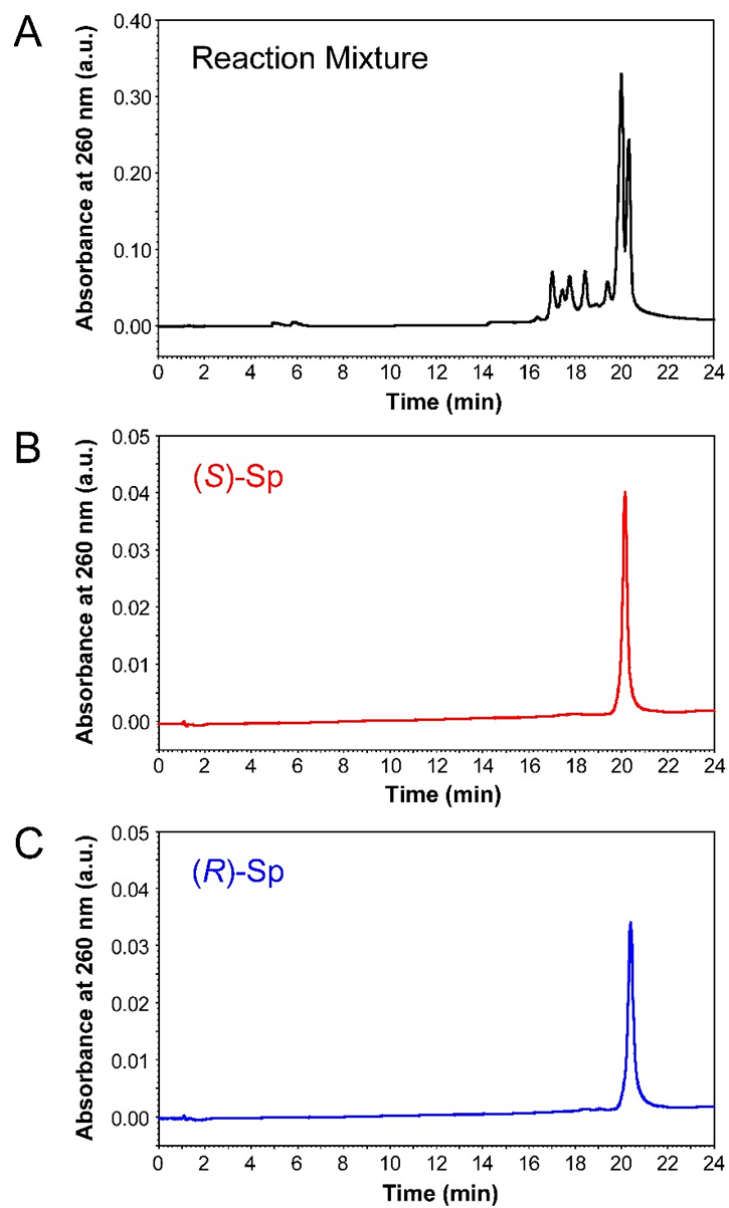


Figure S1. HPLC chromatograms of the reaction mixture (A, black) and the purified oligomers containing (S)-Sp (B, red) or (R)-Sp (C, blue).

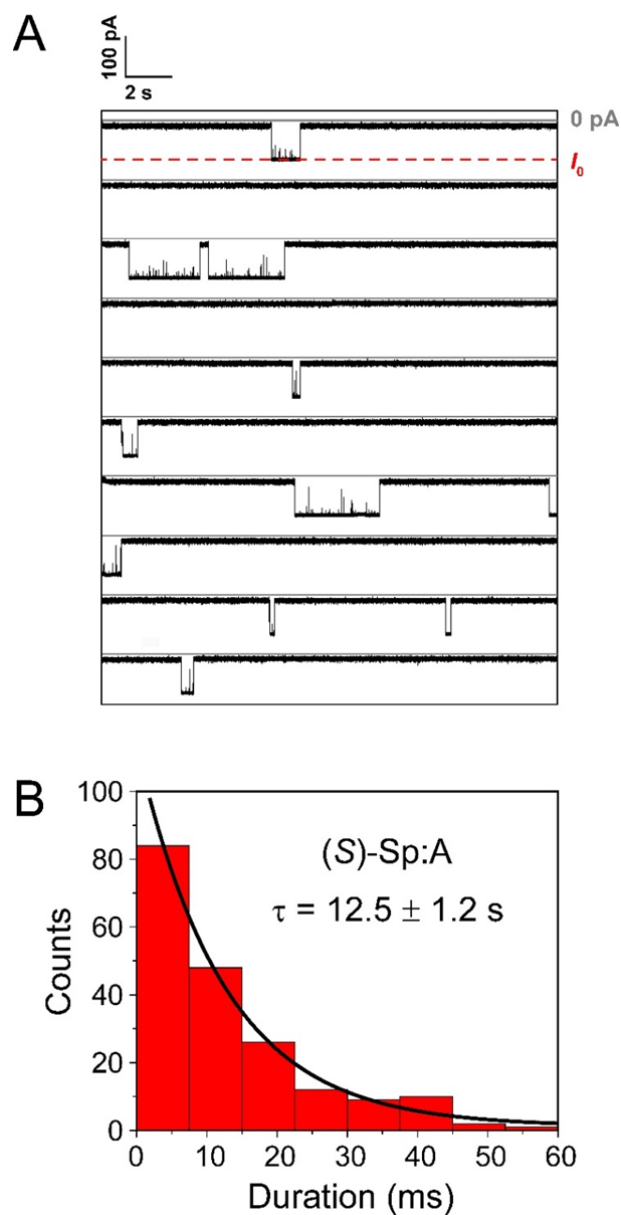


Figure S2. Uninterrupted i - t trace (A) and corresponding duration histogram (B) for (S)-Sp:A-containing duplex in the α HL nanopore. The unzipping lifetime (τ) was obtained by fitting the duration histogram (B) with a first order exponential decay function (the error is based on three individual experiments, in which each experiment comprised over 200 events). Typically, the duplex structure stays inside the α HL channel for tens of seconds before unzipping. The traces were recorded in 1.00 M KCl, 10 mM KP_i , pH 7.4 at 100 mV (*trans* vs. *cis*) and 22 ± 1 °C.

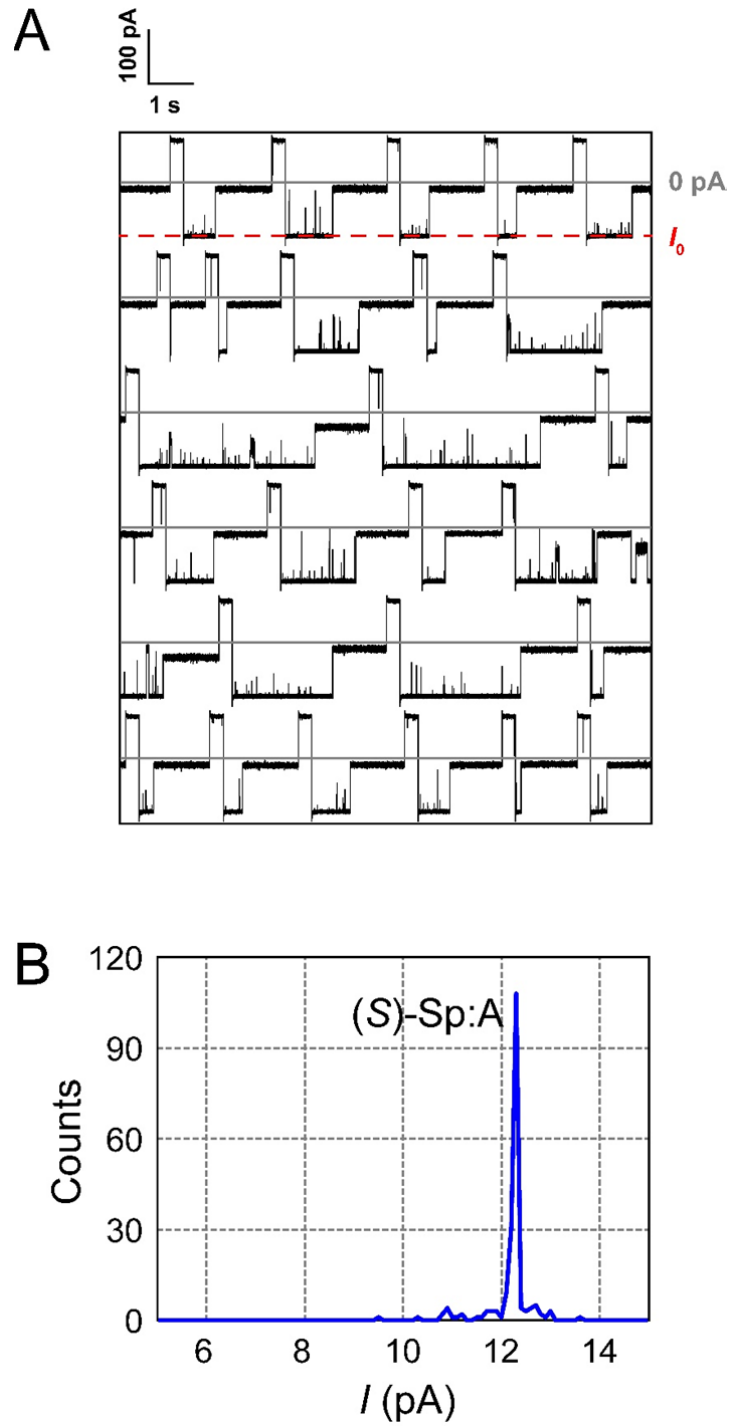


Figure S3. Representative i - t trace (A) and current histogram (B) for (S)-Sp:A-containing duplex in the α HL nanopore. The single peak in the current histogram supports a predominant base pairing configuration between (S)-Sp and A. The traces were recorded in 1.00 M KCl, 10 mM KP_i , pH 7.4 at 100 mV (*trans* vs. *cis*) and 22 ± 1 °C.

Table S1. Current blocks normalized by the open channel current. The data were obtained in 1.00 M KCl, 10 mM KPi, pH 7.4 at 100 mV (*trans* vs. *cis*) and 22 ± 1 °C.

Analyte	$\Delta I/I_0$
(<i>R</i>)-Sp:A vs. (<i>S</i>)-Sp:A	0.004 ± 0.001
(<i>R</i>)-Sp:G vs. (<i>S</i>)-Sp:G	0.008 ± 0.001
(<i>R</i>)-Sp:T vs. (<i>S</i>)-Sp:T	0.004 ± 0.001
(<i>R</i>)-Sp:C vs. (<i>S</i>)-Sp:C	0.003 ± 0.001
(<i>S</i>)-Sp:A vs. T:A	0.026 ± 0.001
(<i>R</i>)-Sp:A vs. T:A	0.029 ± 0.001
(<i>S</i>)-Sp:G vs. T:A	0.022 ± 0.002
(<i>R</i>)-Sp:G vs. T:A	0.029 ± 0.001
(<i>S</i>)-Sp:T vs. T:A	0.022 ± 0.002
(<i>R</i>)-Sp:T vs. T:A	0.025 ± 0.002
(<i>S</i>)-Sp:C vs. T:A	0.021 ± 0.001
(<i>R</i>)-Sp:C vs. T:A	0.022 ± 0.001

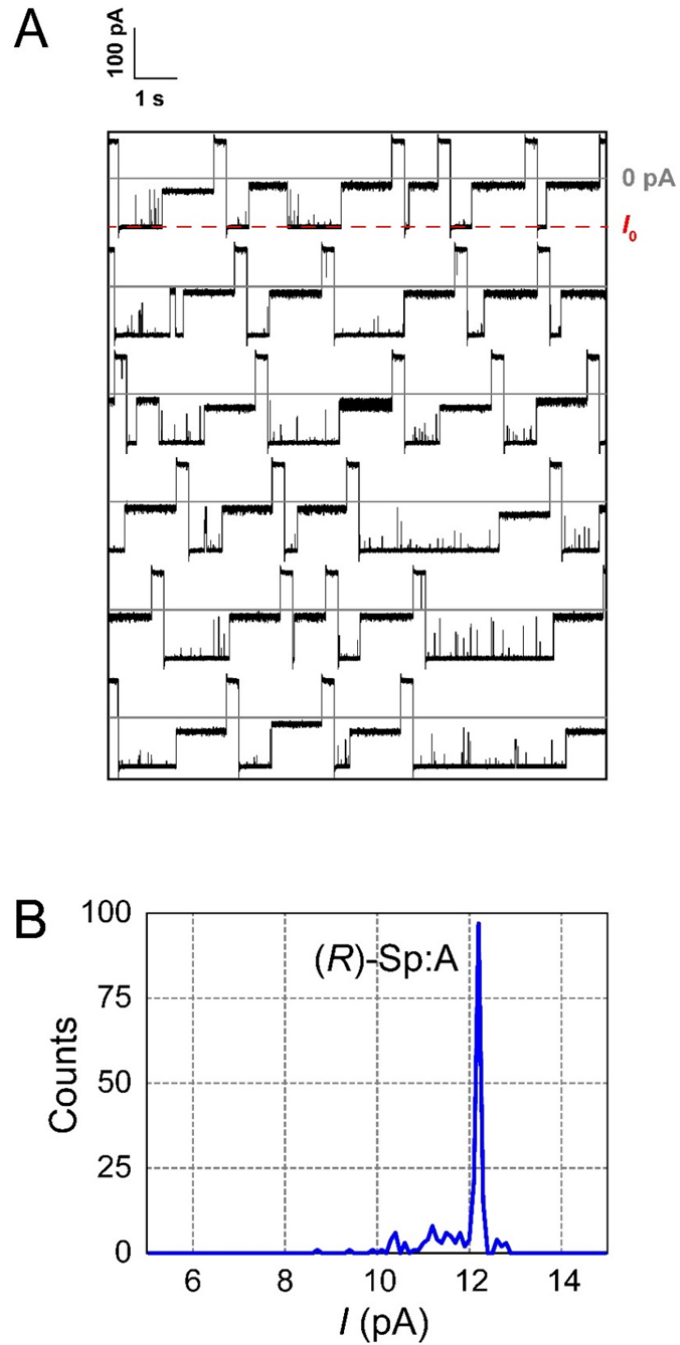


Figure S4. Representative i - t trace (A) and current histogram (B) for (R)-Sp:A-containing duplex in the α HL nanopore. The single peak in the current histogram supports a predominant base pairing configuration between (R)-Sp and A, similar to the base pair S-Sp:A (Figure S3). The traces were recorded in 1.00 M KCl, 10 mM KP_i , pH 7.4 at 100 mV (*trans* vs. *cis*) and 22 ± 1 °C.

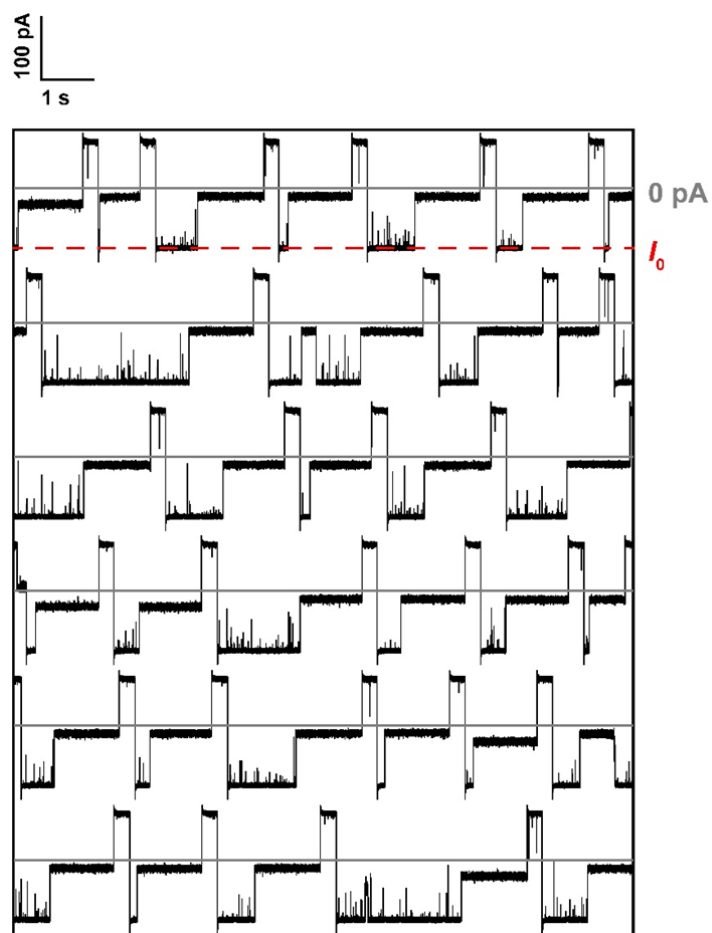


Figure S5. Additional sample of $i-t$ trace for a mixture of (S)-Sp:A- and (R)-Sp:A-containing duplexes in the α HL nanopore. The traces were recorded in 1.00 M KCl, 10 mM KPi , pH 7.4 at 100 mV (*trans* vs. *cis*) and 22 ± 1 °C. These data were used to construct the current histogram and current-noise density plot shown in Figure 4C and Figure 4D of the main text.

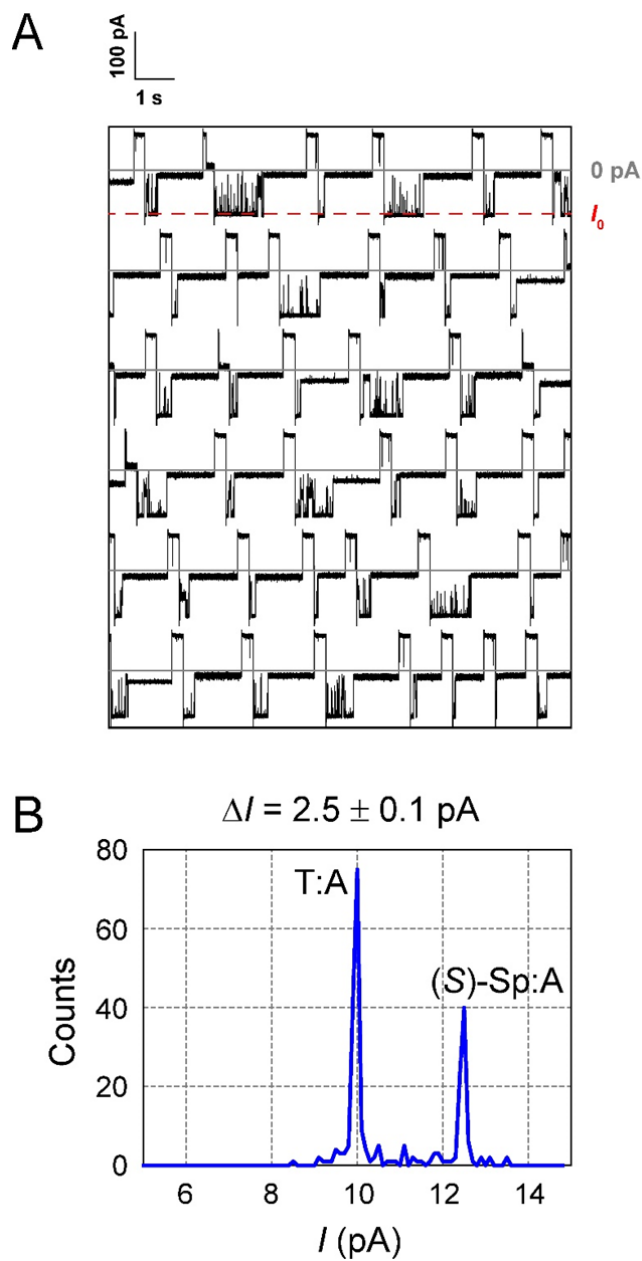


Figure S6. Representative i - t trace (A) and current histogram (B) for (S)-Sp:A-containing duplex vs. the T:A internal standard in the α HL nanopore. The 2:1 peak ratio reflects the twofold greater concentration of the T:A standard. The current difference between (S)-Sp:A duplex and the T:A internal standard is 2.5 ± 0.1 pA (the error is based on three individual experiments, in which each experiment comprised over 200 events). The traces were recorded in 1.00 M KCl, 10 mM KP_i , pH 7.4 at 100 mV (*trans* vs. *cis*) and 22 ± 1 °C.

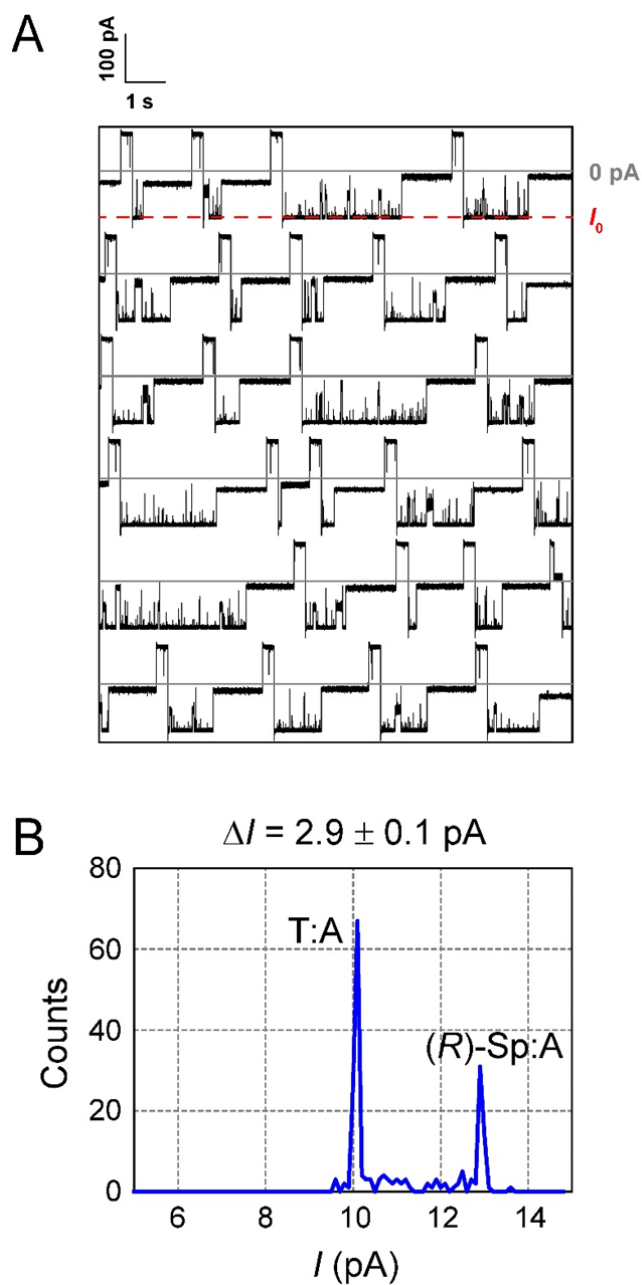


Figure S7. Representative i - t trace (A) and current histogram (B) for (R)-Sp:A-containing duplex vs. the T:A internal standard in the α HL nanopore. The 2:1 peak ratio reflects the twofold greater concentration of the T:A standard. The current difference between (R)-Sp:A duplex and the T:A internal standard is 2.9 ± 0.1 pA (the error is based on three individual experiments, in which each experiment comprised over 200 events). The traces were recorded in 1.00 M KCl, 10 mM KP_i , pH 7.4 at 100 mV (*trans* vs. *cis*) and 22 ± 1 °C.

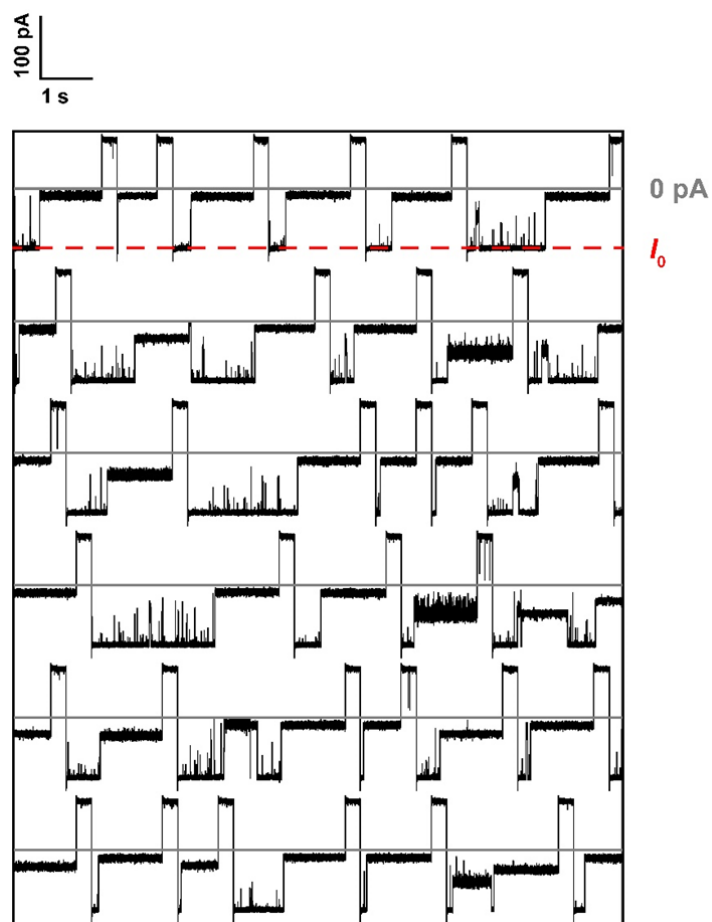


Figure S8. Representative i - t trace for a mixture of (S)-Sp:G- and (R)-Sp:G-containing duplexes in the α HL nanopore. The traces were recorded in 1.00 M KCl, 10 mM KP_i , pH 7.4 at 100 mV (*trans* vs. *cis*) and 22 ± 1 °C. These data were used to construct the current histogram shown in Fig 5A of the main text.

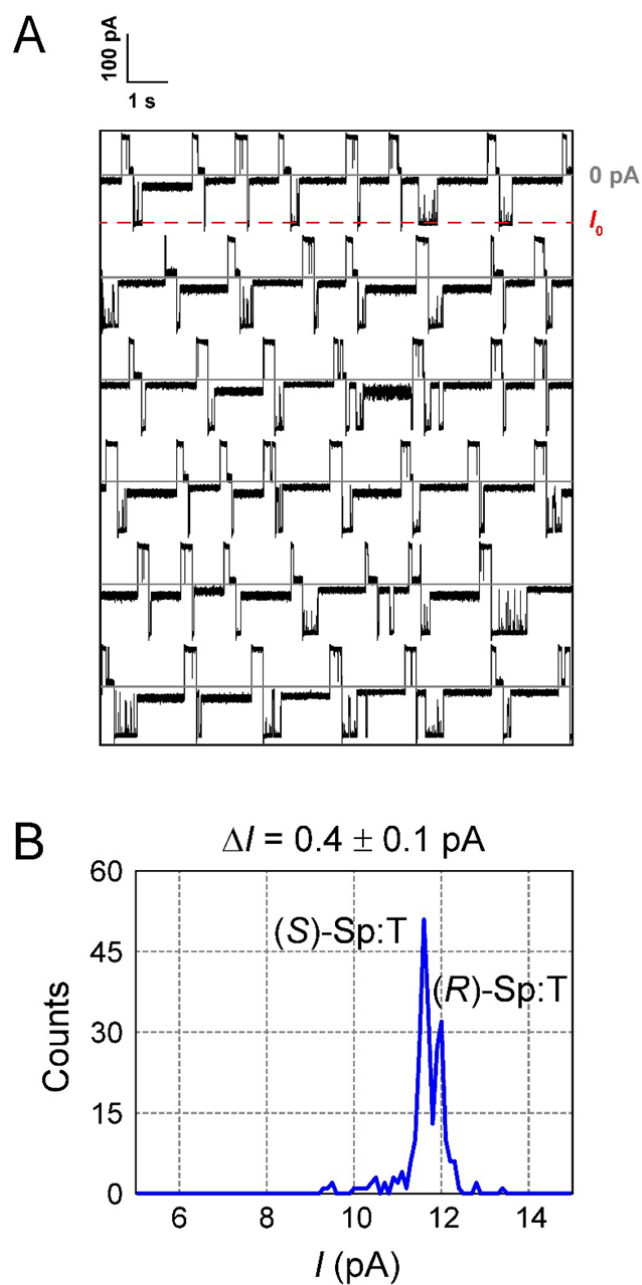


Figure S9. Representative i - t trace (A) and current histogram (B) for a mixture of (S)-Sp:T- and (R)-Sp:T-containing duplexes in the α HL nanopore. The 2:1 peak ratio reflects the twofold greater concentration of (S)-Sp:T duplex. The current difference between (S)-Sp:T and (R)-Sp:T duplexes is 0.4 ± 0.1 pA (the error is based on three individual experiments, in which each experiment comprised over 200 events). The traces were recorded in 1.00 M KCl, 10 mM KP_i , pH 7.4 at 100 mV (*trans* vs. *cis*) and 22 ± 1 °C.

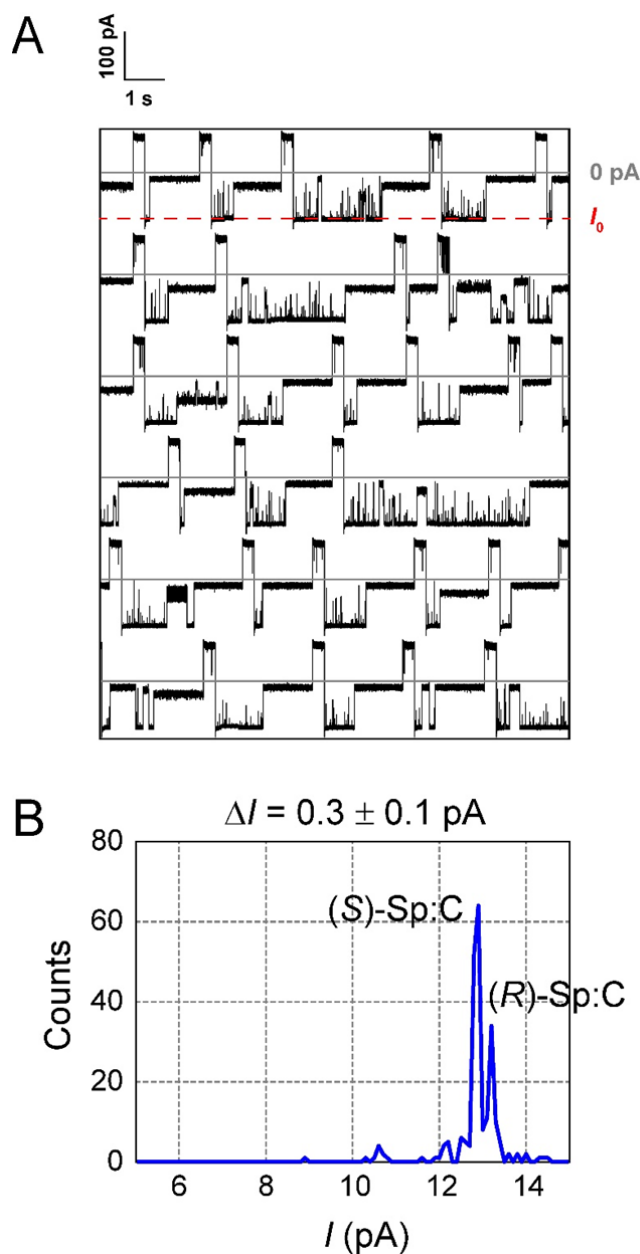


Figure S10. Representative $i-t$ trace (A) and current histogram (B) for a mixture of (S)-Sp:C- and (R)-Sp:C-containing duplexes in the α HL nanopore. The 2:1 peak ratio reflects the twofold greater concentration of (S)-Sp:C duplex. The current difference between (S)-Sp:C and (R)-Sp:C duplexes is 0.3 ± 0.1 pA (the error is based on three individual experiments, in which each experiment comprised over 200 events). The traces were recorded in 1.00 M KCl, 10 mM KP_i , pH 7.4 at 100 mV (*trans* vs. *cis*) and 22 ± 1 °C.

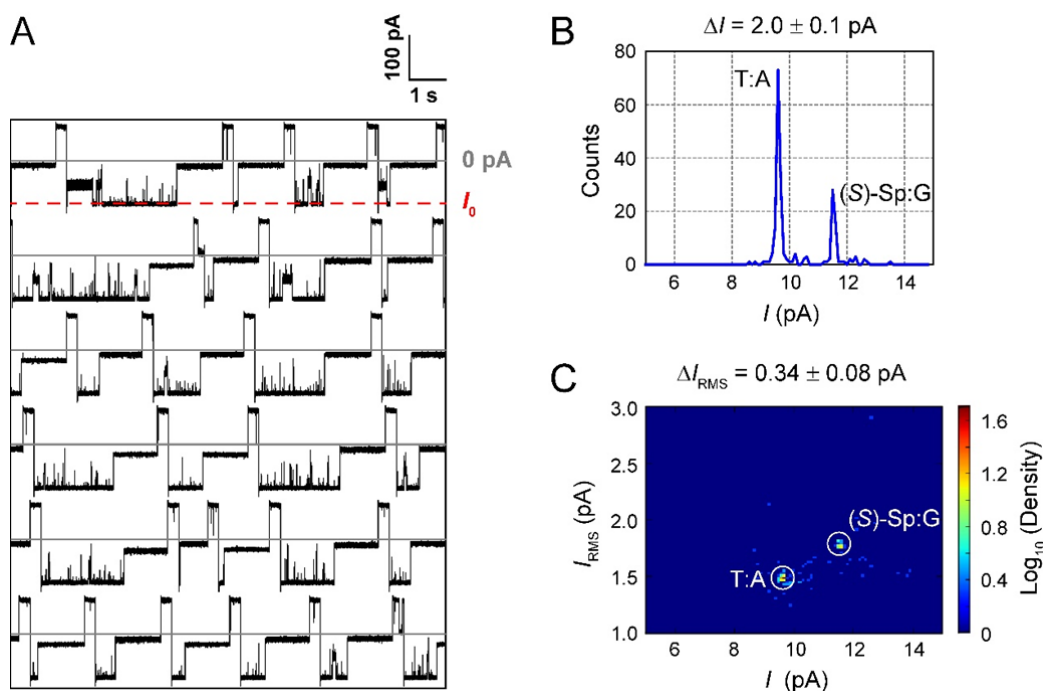


Figure S11. Representative $i-t$ trace (A), current histogram (B), and current-noise density plot (C) for (S)-Sp:G-containing duplex vs. the T:A internal standard in the α HL nanopore. The 2:1 peak ratio in the current histogram reflects the twofold greater concentration of the T:A standard. The current (B) and noise (C) differences between (S)-Sp:G duplex and the T:A internal standard are 2.0 ± 0.1 pA and 0.34 ± 0.08 pA, respectively (the errors are based on three individual experiments, in which each experiment comprised over 200 events). The traces were recorded in 1.00 M KCl, 10 mM KP_i , pH 7.4 at 100 mV (*trans* vs. *cis*) and 22 ± 1 °C.

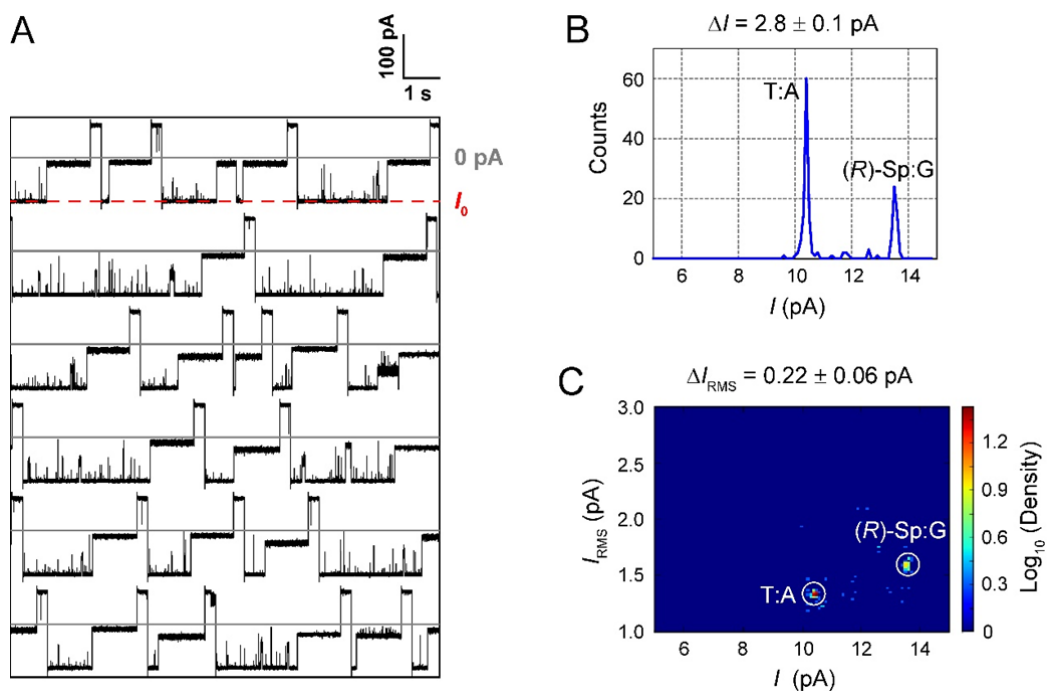


Figure S12. Representative $i-t$ trace (A), current histogram (B), and current-noise density plot (C) for R -Sp:G-containing duplex vs. the T:A internal standard in the α HL nanopore. The 2:1 peak ratio in the current histogram reflects the twofold greater concentration of the T:A standard. The current (B) and noise (C) differences between R -Sp:G duplex and the T:A internal standard are 2.8 ± 0.1 pA and 0.22 ± 0.06 pA, respectively (the errors are based on three individual experiments, in which each experiment comprised over 200 events). The traces were recorded in 1.00 M KCl, 10 mM KP_i , pH 7.4 at 100 mV (*trans* vs. *cis*) and 22 ± 1 °C.

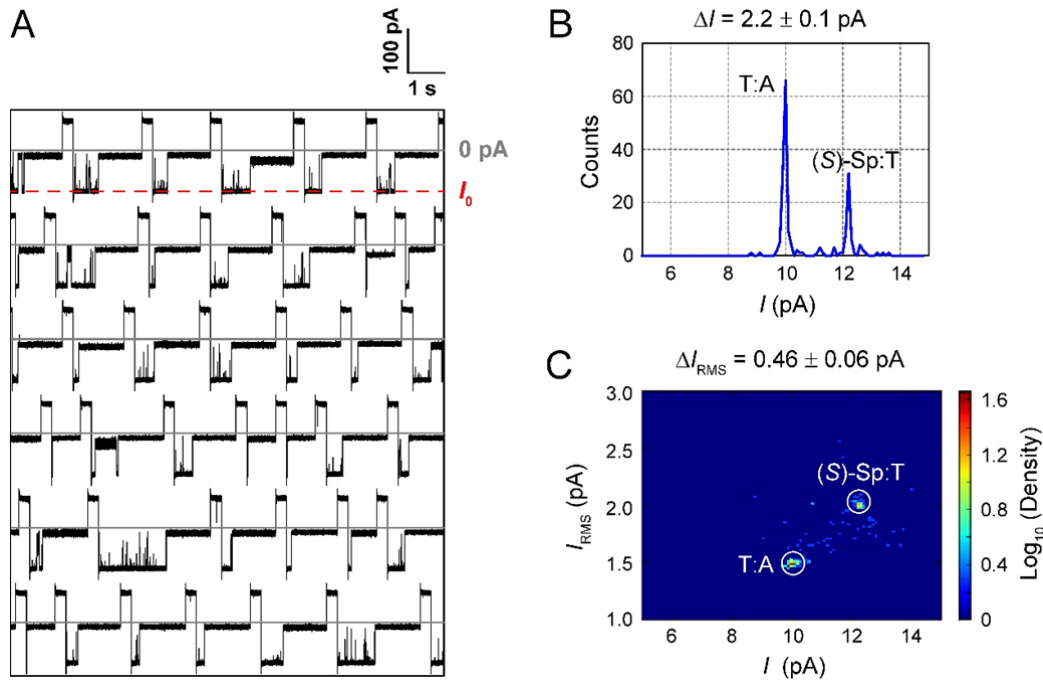


Figure S13. Representative $i-t$ trace (A), current histogram (B), and current-noise density plot (C) for (S)-Sp:T-containing duplex vs. the T:A internal standard in the α HL nanopore. The 2:1 peak ratio in the current histogram reflects the twofold greater concentration of the T:A standard. The current (B) and noise (C) differences between (S)-Sp:T duplex and the T:A internal standard are 2.2 ± 0.1 pA and 0.46 ± 0.06 pA, respectively (the errors are based on three individual experiments, in which each experiment comprised over 200 events). The traces were recorded in 1.00 M KCl, 10 mM KP_i , pH 7.4 at 100 mV (*trans* vs. *cis*) and 22 ± 1 °C.

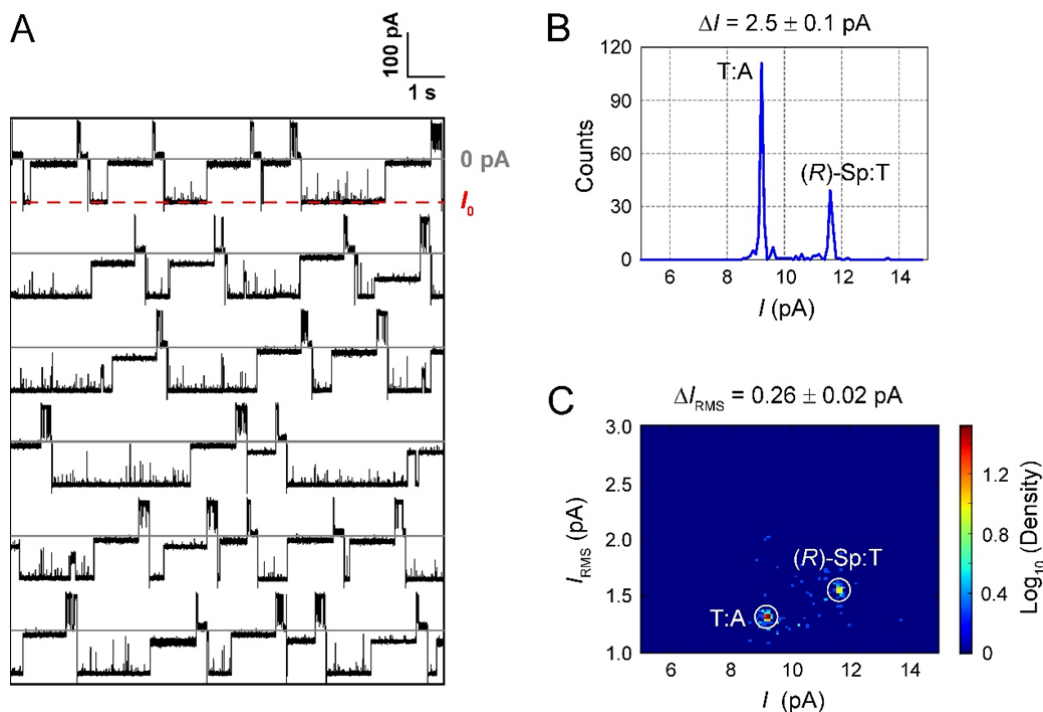


Figure S14. Representative $i-t$ trace (A), current histogram (B), and current-noise density plot (C) for (R)-Sp:T-containing duplex vs. the T:A internal standard in the α HL nanopore. The 2:1 peak ratio in the current histogram reflects the twofold greater concentration of the T:A standard. The current (B) and noise (C) differences between (R)-Sp:T duplex and the T:A internal standard are 2.5 ± 0.1 pA and 0.26 ± 0.02 pA, respectively (the errors are based on three individual experiments, in which each experiment comprised over 200 events). The traces were recorded in 1.00 M KCl, 10 mM KP_i , pH 7.4 at 100 mV (*trans* vs. *cis*) and 22 ± 1 °C.

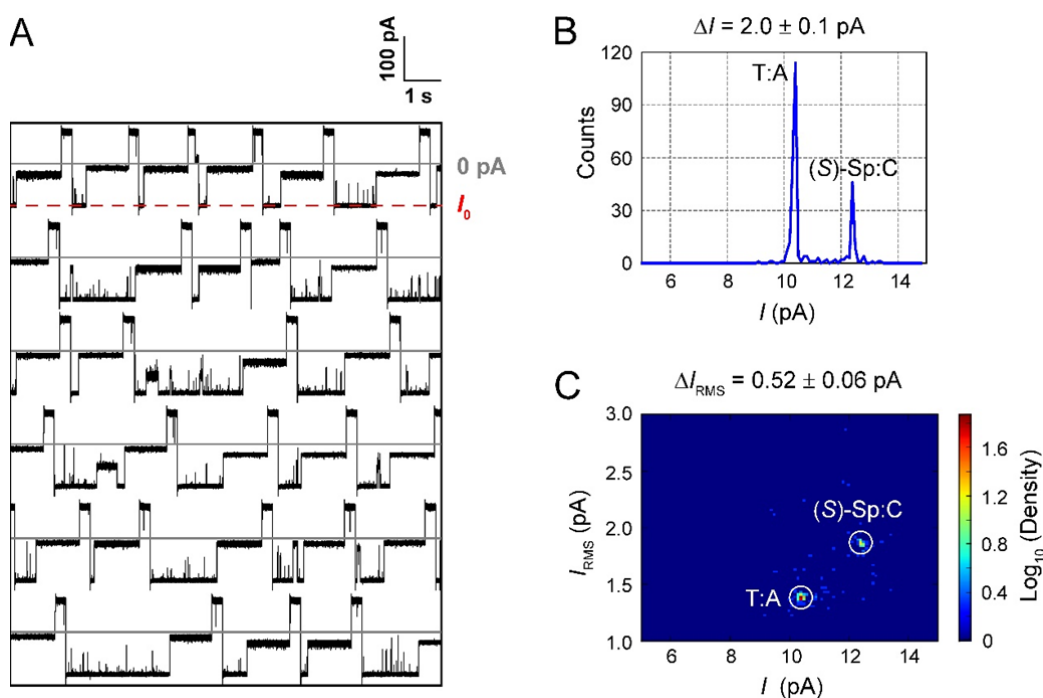


Figure S15. Representative $i-t$ trace (A), current histogram (B), and current-noise density plot (C) for (S)-Sp:C-containing duplex vs. the T:A internal standard in the α HL nanopore. The 2:1 peak ratio in the current histogram reflects the twofold greater concentration of the T:A standard. The current (B) and noise (C) differences between (S)-Sp:C duplex and the T:A internal standard are 2.0 ± 0.1 pA and 0.52 ± 0.06 pA, respectively (the errors are based on three individual experiments, in which each experiment comprised over 200 events). The traces were recorded in 1.00 M KCl, 10 mM KP_i , pH 7.4 at 100 mV (*trans* vs. *cis*) and 22 ± 1 °C.

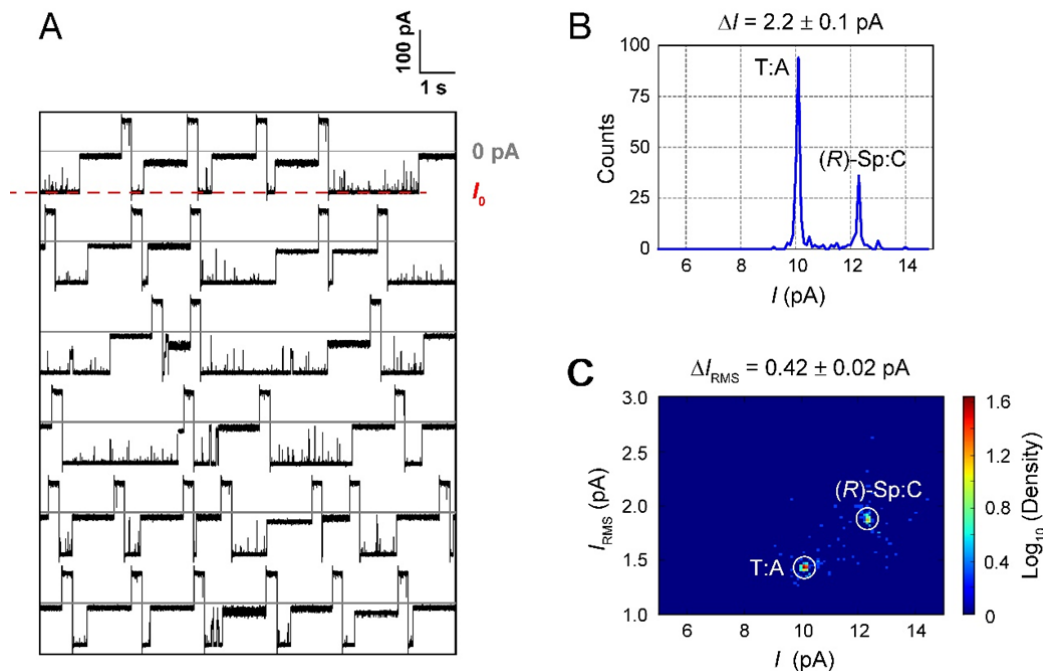


Figure S16. Representative $i-t$ trace (A), current histogram (B), and current-noise density plot (C) for (R)-Sp:C-containing duplex vs. the T:A internal standard in the α HL nanopore. The 2:1 peak ratio in the current histogram reflects the twofold greater concentration of the T:A standard. The current (B) and noise (C) differences between (R)-Sp:C duplex and the T:A internal standard are 2.2 ± 0.1 pA and 0.42 ± 0.02 pA, respectively (the errors are based on three individual experiments, in which each experiment comprised over 200 events). The traces were recorded in 1.00 M KCl, 10 mM KP_i , pH 7.4 at 100 mV (*trans* vs. *cis*) and 22 ± 1 °C.

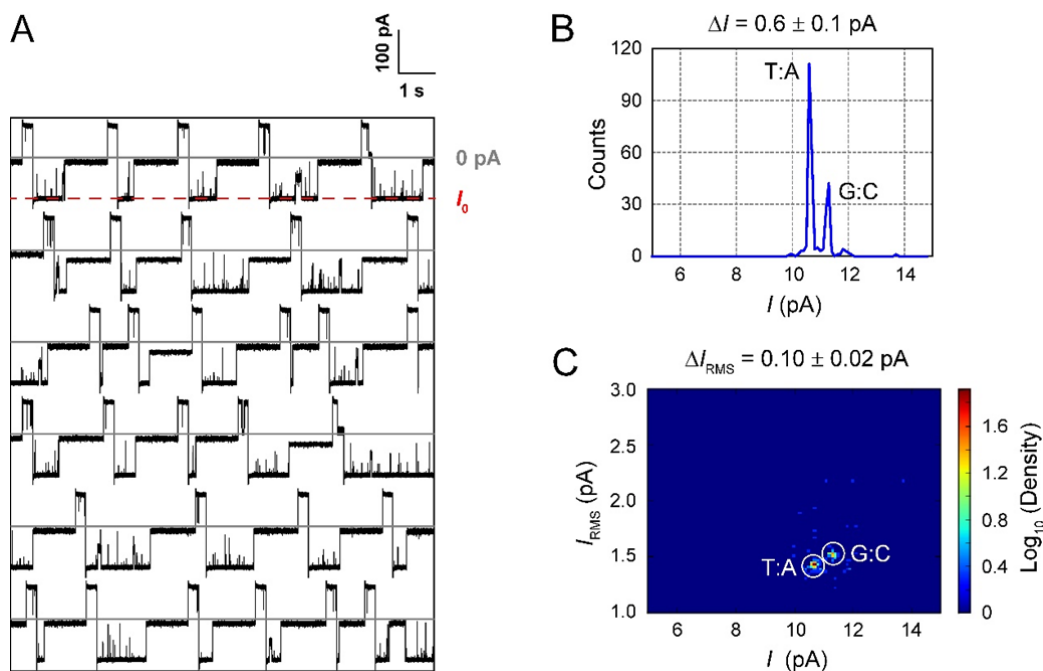


Figure S17. Representative $i-t$ trace (A), current histogram (B), and current-noise density plot (C) for G:C-containing duplex vs. the T:A internal standard in the α HL nanopore. The 2:1 peak ratio in the current histogram reflects the twofold greater concentration of the T:A standard. The current (B) and noise (C) differences between G:C duplex and the T:A internal standard are 0.6 ± 0.1 pA and 0.10 ± 0.02 pA, respectively (the errors are based on three individual experiments, in which each experiment comprised over 200 events). The traces were recorded in 1.00 M KCl, 10 mM KPi , pH 7.4 at 100 mV (*trans* vs. *cis*) and 22 ± 1 °C.

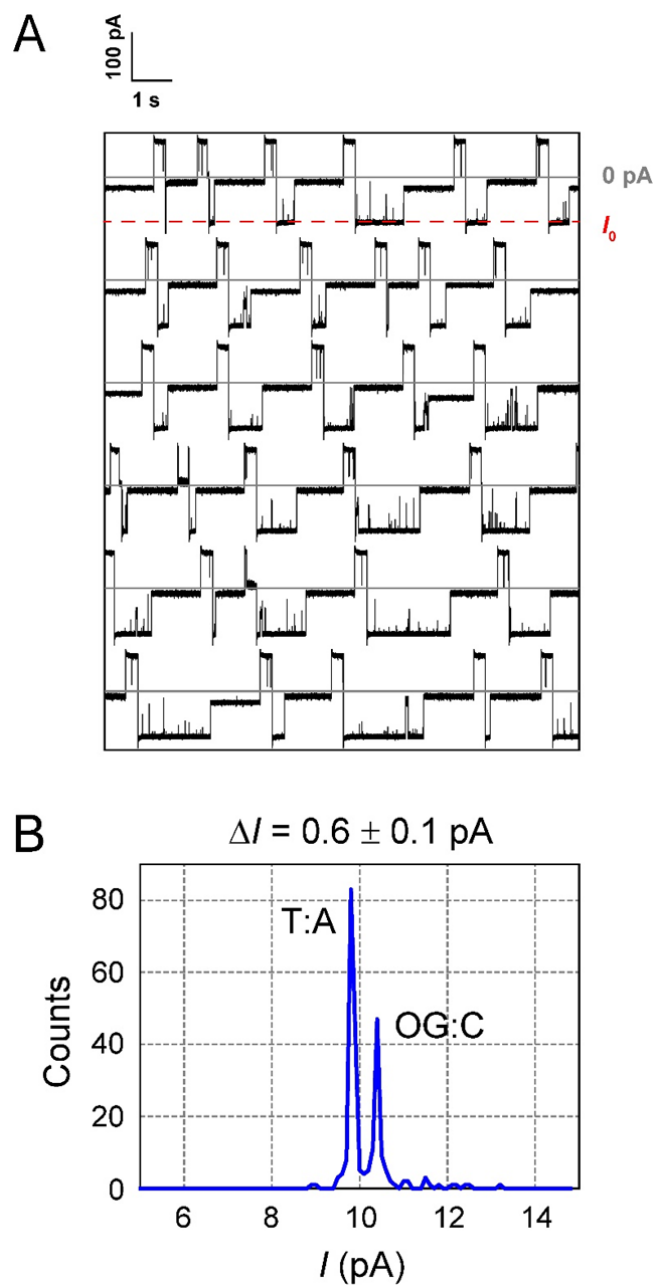


Figure S18. Representative i - t trace (A) and current histogram (B) for OG:C-containing duplex vs. the T:A internal standard in the α HL nanopore. The 2:1 peak ratio reflects the twofold greater concentration of the T:A standard. The current difference between OG:C duplex and the T:A internal standard is 0.6 ± 0.1 pA (the error is based on three individual experiments, in which each experiment comprised over 200 events). The traces were recorded in 1.00 M KCl, 10 mM KP_i , pH 7.4 at 100 mV (*trans* vs. *cis*) and 22 ± 1 °C.

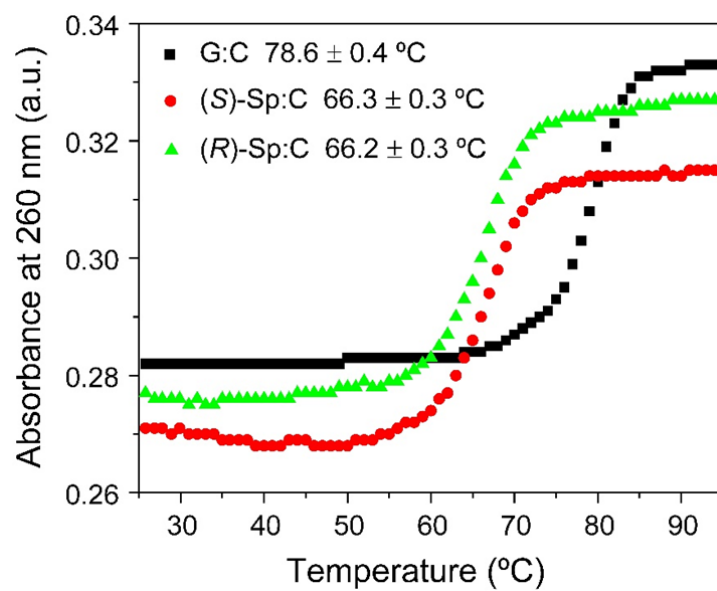


Figure S19. Melting curves for the duplexes containing G:C (black square), (S)-Sp:C (red circle), or (R)-Sp:C (green triangle) base pair. The data were collected in 1.00 M KCl, 10 mM KPi, pH 7.4 with a DNA concentration of 0.75 μ M. Note that the (CAT)₁₀ tail was removed from the sequences in the T_m experiments.